OCEAN ACIDIFICATION NEWS

How community interactions amplify response of calcifying phytoplankton species to ocean acidification

Summary: Coccolithophores, single-celled calcifying phytoplankton that play a key role in the Earth's climate system, might lose their competitive fitness in a future ocean. In a field experiment investigating the effects of ocean acidification on the coccolithophore Emiliania huxleyi in its natural environment, the species failed to bloom. A team of researchers concludes, that a small response to ocean acidification was amplified through ecological interactions and causes a massive impact on the ecosystem.

The uptake of fossil fuel carbon dioxide (CO_2) by the ocean increases seawater acidity and causes a decline in carbonate ion concentrations. This process, termed ocean acidification, makes it energetically more costly for calcifying organisms to form their calcareous shells and skeletons. Several studies have shown that this also holds true for *Emiliania huxleyi*, the world's most abundant and most productive calcifying organism. When exposed to ocean acidification in controlled laboratory experiments, growth and calcification rates of the single-celled alga are slightly reduced. Even after more than two thousand generations under acidified conditions, these responses still prevail to some extent, suggesting that evolutionary adaptation may not be able to completely eliminate the negative effects of ocean acidification. But what this means in terms of the alga's ability to maintain competitive fitness in its natural environment when the ocean continues to acidify was still an open question.

To address this question, a team of researchers led by GEOMAR Helmholtz Centre for Ocean Research Kiel conducted a field experiment using the KOSMOS (Kiel Off-Shore Mesocosms for Ocean Simulations) experimental platform. As part of the research projects SOPRAN (Surface Ocean Processes in the Anthropocene) and BIOACID (Biological Impacts of Ocean Acidification) the KOSMOS system was deployed in the Raunefjord at the west coast of Norway, were blooms of *Emiliania huxleyi* regularly occur in late spring. Each of the nine KOSMOS units enclosed about 75 cubic metres of seawater in a 25 metres long plastic bag. The "giant test tubes" were brought to carbon dioxide concentrations ranging from present to projected mid-of-next-century levels. For six weeks, the scientists measured various parameters and took samples for further analyses. Sinking particles were collected in funnel-shaped sediment traps at the lower end of the mesocosms and analysed as well.

In view of *Emiliania*'s rather small changes in metabolic performance observed in previous laboratory experiments, we predicted that it would still be able to maintain its ecological niche in an acidifying ocean. What we observed came as a big surprise, says Prof. Ulf Riebesell, marine biologist at GEOMAR Helmholtz Centre for Ocean Research Kiel and coordinator of the KOSMOS experiments. In the mesocosms simulating future ocean conditions, *Emiliania* failed to form a bloom. Detailed analysis of the data revealed that *Emiliania*'s downfall started well before the bloom period. A small reduction in cellular growth due to ocean acidification caused the population size to gradually decline during the pre-bloom phase. "When it was time for *Emiliania* to start bloom formation, there were so few cells left in the plankton community that it couldn't outgrow its competitors anymore," reflects Ulf Riebesell.

The loss of competitive fitness in the calcifying alga had strong impacts on the ecosystem. The flux of organic matter to depth was strongly reduced in the absence of bloom formation, explains Dr. Kai Schulz, marine biogeochemist at Southern Cross University, Australia. The reason is that *Emiliania*'s dense calcareous platelets function as ballast in aggregated organic matter and accelerate its sinking to the deep ocean. Without the chalky ballast the aggregates sink more slowly and bacteria have more time to degrade the organic matter in the surface layer. As a result of this, more of the CO_2 bound in organic matter remains in the surface layer, which reduces the ocean's potential to take up atmospheric CO_2.

Another feedback could result from the fact that *Emiliania* is one of the dominant producers of dimethylsulfide, a volatile gas which is thought to serve as cooling agent in the climate system. Whereas high concentrations of this gas were recorded in the mesocosms were *Emiliania* was blooming, they were greatly reduced in the mesocosms simulating future conditions. Less CO_2 uptake by the ocean and lower production of the cooling agent dimethylsulfide would both work in the same direction, reducing the ocean's capacity to mitigate global warming.

The results of this study demonstrate the importance of investigating the effects of ocean acidification in natural communities. Small changes in an organism's metabolic performance can have major consequences for its success in its natural habitat, where it is in competition with other species and faces losses from predation or viral infection. If *Emiliania huxleyi* fails to maintain its important role, other, possibly non-calcifying, organisms take over. This might initiate a regime shift with far-reaching ecological and biogeochemical consequences, Prof. Riebesell concludes.

Journal Reference: Ulf Riebesell, Lennart T. Bach, Richard G. J. Bellerby, J. Rafael Bermúdez Monsalve, Tim Boxhammer, Jan Czerny, Aud Larsen, Andrea Ludwig, Kai G. Schulz. **Competitive fitness of a predominant pelagic calcifier impaired by ocean acidification**. *Nature Geoscience*, 2016; DOI: 10.1038/ngeo2854

Competitive fitness of a predominant pelagic calcifier impaired by ocean acidification

Ulf Riebesell[1]*, Lennart T. Bach[1], Richard G. J. Bellerby[2,3], J. Rafael Bermúdez Monsalve[1,4], Tim Boxhammer[1], Jan Czerny[1], Aud Larsen[5], Andrea Ludwig[1] and Kai G. Schulz[6]

Coccolithophores—single-celled calcifying phytoplankton—are an important group of marine primary producers and the dominant builders of calcium carbonate globally. Coccolithophores form extensive blooms and increase the density and sinking speed of organic matter via calcium carbonate ballasting. Thereby, they play a key role in the marine carbon cycle. Coccolithophore physiological responses to experimental ocean acidification have ranged from moderate stimulation to substantial decline in growth and calcification rates, combined with enhanced malformation of their calcite platelets. Here we report on a mesocosm experiment conducted in a Norwegian fjord in which we exposed a natural plankton community to a wide range of CO_2-induced ocean acidification, to test whether these physiological responses affect the ecological success of coccolithophore populations. Under high-CO_2 treatments, *Emiliania huxleyi*, the most abundant and productive coccolithophore species, declined in population size during the pre-bloom period and lost the ability to form blooms. As a result, particle sinking velocities declined by up to 30% and sedimented organic matter was reduced by up to 25% relative to controls. There were also strong reductions in seawater concentrations of the climate-active compound dimethylsulfide in CO_2-enriched mesocosms. We conclude that ocean acidification can lower calcifying phytoplankton productivity, potentially creating a positive feedback to the climate system.

Large parts of the ocean regularly experience extensive blooms of coccolithophores, which can be easily seen from space when cells shed their calcite platelets making the waters appear milky[1]. While the costs and benefits of calcification in coccolithophores are still uncertain[2,3], its crucial role in ocean biogeochemistry is well documented. Coccolithophores are responsible for about half of pelagic calcium carbonate production[4], which increases Earth's albedo[5], decreases oceanic CO_2 uptake through the reduction of surface layer alkalinity[6], and enhances carbon flux to depth by providing calcite ballast to accelerate sinking of organic particles[7,8]. As with other calcareous organisms, calcification in coccolithophores is expected to become energetically more costly as the ocean continues to acidify due to anthropogenic CO_2 uptake[9]. Studies on the physiological performance of coccolithophores under future ocean scenarios revealed strain- and species-specific variations[10,11]. While some species showed no detectable change in calcification, photosynthesis and growth rate when exposed to elevated CO_2/reduced pH, others responded with a 10 to 50% decline in calcification and a 10 to 20% increase in photosynthesis[12]. Among these, the bloom-forming *Emiliania huxleyi* proved to be moderately sensitive, with an average 25% decrease in calcification rate and no significant change in photosynthesis in response to projected year 2100 ocean acidification levels. However, key questions remain about how physiological responses affect the ecological success of coccolithophores and whether potential changes in coccolithophore competitiveness feed back on key biogeochemical processes such as carbon export or the release of climate-relevant trace gases.

Mesocosm setup and plankton community succession

To address these questions we performed an *in situ* mesocosm study at the west coast of southern Norway, an area that experiences extensive annual blooms of *E. huxleyi* in the late spring/early summer. Nine 25-m-long, pelagic mesocosms, each enclosing about 75 m^3 of seawater, were deployed in the Raunefjord at 60.265° N, 5.205° E on 30 April 2011 (Supplementary Fig. 1). The carbonate chemistry of the enclosed seawater was manipulated by stepwise additions of CO_2-saturated seawater over 5 days. p_{CO_2} and pH$_T$ initially covered a range from ∼300 to ∼3,000 µatm and from 8.14 to 7.2, respectively. While the two highest CO_2 levels fall well outside the range projected for this century and beyond, they were chosen to serve as 'proof of concept' while keeping the majority of mesocosms in the range of representative concentration pathway scenarios of the Intergovernmental Panel on Climate Change's Fifth Assessment Report[13]. Outgassing of CO_2 caused a gradual p_{CO_2} decline (Fig. 1a) and pH$_T$ increase in CO_2-enriched mesocosms. Sampling of the mesocosms and the surrounding fjord started on 7 May, one day before the first CO_2 addition (termed 'day 0'). On day 14, 5 µmol l^{-1} nitrate and 0.16 µmol l^{-1} phosphate were added to the mesocosms.

Inorganic nutrients available in the fjord water at the time of mesocosm closing were utilized by pico- and nano-phytoplankton, the latter dominated by the diatom *Arcocellulus cornucervis*, leading to a first bloom between days 3 and 5 (Fig. 1b). The nutrients added on day 14 stimulated net growth of phytoplankton, leading to a second biomass increase, again primarily by pico- and nano-phytoplankton, dominated by chlorophytes, cryptophytes and the diatom *A. cornucervis*. In the waters surrounding the mesocosms,

Figure 1 | Time course of key parameters in the mesocosms.
a–d, p_{CO_2} (**a**), chlorophyll *a* concentration (**b**), cell abundances of *E. huxleyi* on a linear scale (**c**) and on a log scale (**d**) in the eight mesocosms during the course of the experiment. Blue, grey and red colours represent low ($p_{CO_2} < 400\,\mu$atm)-, intermediate (p_{CO_2} 400–1,000 μatm)- and high ($p_{CO_2} > 1,000\,\mu$atm)-CO$_2$ treatments, respectively. The black coloured symbols and lines represent the adjacent fjord waters. The vertical line indicates the time of nutrient addition on day 14.

phytoplankton biomass followed a similar pattern with lower peak values and preceding those in the mesocosms by 4–6 days. While chlorophyll concentrations in the mesocosms correlated positively with p_{CO_2} enrichment during the first bloom (adjusted $R^2 = 0.7598$, $F = 23.14$, $p = 0.003$), the opposite relationship, although not statistically significant (adjusted $R^2 = 0.3536$, $F = 4.83$, $p = 0.070$), occurred during the second bloom.

Response of *Emiliania huxleyi* to ocean acidification

E. huxleyi, present in the fjord and in the mesocosms at the time of closing, remained at low abundances during the first two weeks of the experiment (Fig. 1c). Cell numbers of *E. huxleyi* increased slightly and subsequently decreased concomitant with the build-up and decline of the first phytoplankton bloom (Fig. 1d). *E. huxleyi* abundance started to deviate between CO$_2$ treatments on day 7. While population density remained approximately stable

in the low-CO$_2$ treatments, it continued to decline under high CO$_2$ until day 14, the time of nutrient addition (Fig. 1d). Net growth rate inversely correlated with p_{CO_2} during this period (Fig. 2a and Supplementary Fig. 3) and was negative when p_{CO_2} values exceeded 500 μatm. On day 14, the population density differed up to more than tenfold between low- and high-CO$_2$ treatments and was significantly correlated with p_{CO_2} (Figs 1d and 2c). Following nutrient addition on day 14 and the onset of vertical stratification the day after (day 15), net growth rate of *E. huxleyi* turned positive in all CO$_2$ treatments, but remained lower, although not significantly, under high-CO$_2$ conditions (Fig. 2b). Whereas a moderate bloom developed in three of the lowest CO$_2$ treatments, population densities remained low in all other mesocosms (Figs 1c and 2d). Peak cell densities of 1.5–3×10^6 cells l^{-1}, both in the fjord and in the mesocosms, are in the lower range of bloom densities for this species[14]. Interestingly, the increase in *E. huxleyi* abundance occurred at the same time that its abundance increased also in the fjord outside the mesocosms. As concentrations of inorganic nutrients in the fjord water did not change substantially throughout the experiment (Supplementary Fig. 2), the timing of bloom development of *E. huxleyi* in the fjord was probably stimulated by the onset of thermal stratification of the water column. In the mesocosms, nutrient addition shortly before the onset of stratification further supported the increase in *E. huxleyi* population size.

The failure of bloom formation under elevated CO$_2$ conditions was evidently caused primarily by a diminished seed stock at the onset of bloom development (Figs 1c,d and 2). Whether this was due to increased losses, for example through grazing or viral infection, or whether it was due to decreased cell division rates, cannot be determined with certainty from these data. However, as flow cytometry analyses did not reveal a detectable increase in the abundance of the *E. huxleyi* specific virus EhV throughout the experiment in any of the CO$_2$ treatments, viral infection has probably not been a significant loss factor in this experiment and cannot explain the difference in net growth rate of *E. huxleyi* between CO$_2$ treatments. Furthermore, if enhanced grazing under elevated p_{CO_2} would have been responsible for the observed differences between treatments, this should have been visible also in other phytoplankton groups in the size class of *E. huxleyi*, which was not the case. Thus, we argue that a CO$_2$-induced difference in cell division rate was the most likely cause for the observed differences in net growth rate between CO$_2$ treatments.

Results of previous mesocosm CO$_2$-enrichment experiments during *E. huxleyi* bloom season at the same location in 2001[15,16], 2005[17,18] and 2006[19] are generally consistent with this interpretation (Supplementary Table 1). A tendency towards lower net growth rates of *E. huxleyi* under elevated CO$_2$ was also observed in 2001[16] and 2006[19]. While in the latter study this led to lower peak *E. huxleyi* abundances in response to CO$_2$ enrichment, in 2001 the impact was less clear, a phenomenon also observed in 2005. In both cases, inorganic nutrients were added at the start of the experiment in parallel with CO$_2$ enrichment. This immediately stimulated phytoplankton growth and excluded a p_{CO_2} effect on the seed stock density prior to bloom development. The extended duration of the pre-bloom phases in this and in the 2006 study caused the observed differences in *E. huxleyi* population densities at the onset of bloom development, with the consequence of bloom failure at elevated CO$_2$ levels. As the success of a bloom-forming species such as *E. huxleyi* is determined by both the density of the seed population prior to bloom development and net growth rate during bloom build-up, the conditions simulated during this study probably more accurately mimic the natural environment.

Another difference between the four experiments lies in the depth of the upper mixed layer and hence the light intensities experienced by the enclosed phytoplankton communities
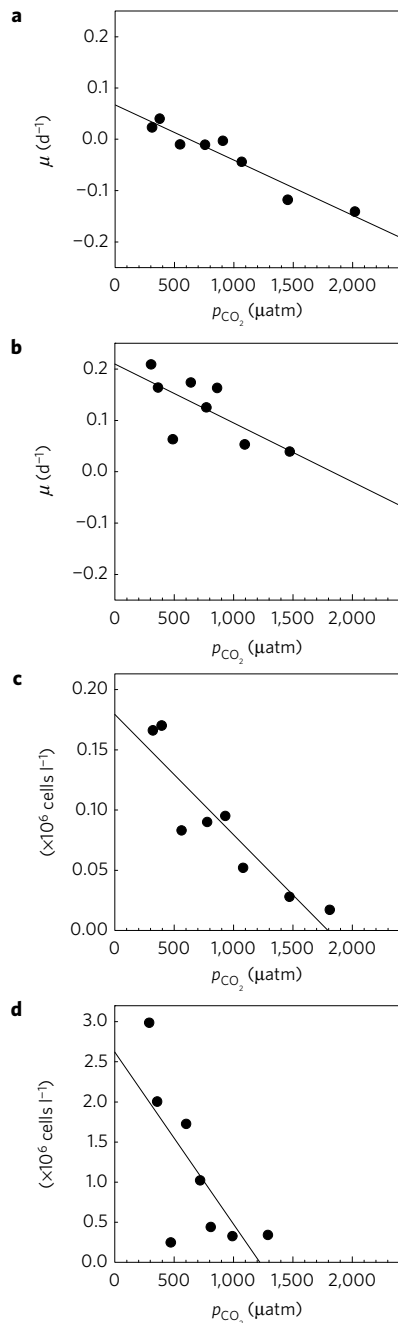
Figure 2 | Responses of *E. huxleyi* to ocean acidification. a,b, Net growth rate of *E. huxleyi* averaged over the period before nutrient addition (days 0–14) (**a**), and between day 15 and the day of maximum cell abundance (**b**), plotted versus p_{CO_2} (µatm) averaged for the respective time periods. **c,d,** *E. huxleyi* cell abundances versus p_{CO_2} on day 14 (**c**), and on the day of maximum cell abundances (**d**). Statistical analysis by Pearson correlation[37] yielded $R^2 = 0.9215$, $p = 0.0002$ (**a**); $R^2 = 0.4949$, $p = 0.0515$ (**b**); $R^2 = 0.8325$, $p = 0.0016$ (**c**); $R^2 = 0.5101$, $p = 0.047$ (**d**). All p values are two-sided.

(Supplementary Table 1). In the 2001 and 2006 experiments, the enclosure depths were 4.5 m (ref. 15) and 3.5 m (ref. 19), respectively. In 2005, the bags used were 9.5 m long, of which the upper 5.7 m were separated from the lower part of the bags by an artificially induced salinity difference between the two layers and continuous mixing of the upper layer[18]. In contrast, the present study was conducted with 25-m-long bags, in which the water column remained non-stratified for at least the first half of the
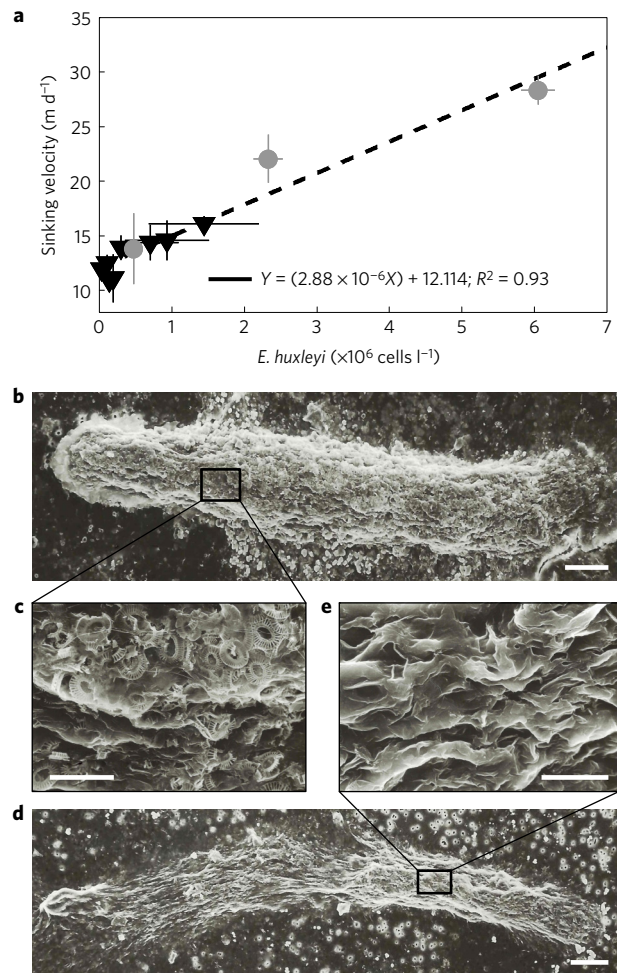
Figure 3 | Effects on sinking particles. a, Sinking velocities of particle aggregates (collected from sediment traps; black triangles) and faecal pellets (produced in triplicate bottle incubations of mesocosm water to which copepods were added; grey circles) as a function of *E. huxleyi* cell abundance ($p \ll 0.01$). Horizontal and vertical error bars show ±1 s.d. **b–e,** Scanning electron micrographs of faecal pellets collected on day 28 in an intermediate-p_{CO_2} mesocosm (M1) (**b,c**), and collected in a high-p_{CO_2} mesocosm (M7) (**d,e**) with large numbers of coccoliths and no coccoliths inside the faecal pellet, respectively. The scale bars represent 30 µm in **b,d** and 6 µm in **c,e**.

experiment. The average light intensities in the upper mixed layers are estimated as 241 and 173 µmol photons $m^{-2} s^{-2}$ for the 2001 and 2005 experiments, respectively, and 56 µmol photons $m^{-2} s^{-2}$ for the present study (Supplementary Table 1). Due to interacting effects of CO_2 and light intensity on coccolithophore performance[20–22], this difference may have contributed to the more pronounced response of *E. huxleyi* in this compared with the previous studies.

Biogeochemical implications

The failure of *E. huxleyi* bloom development under high-CO_2 conditions had major consequences for key biogeochemical processes in the mesocosms. The sinking rates of particle aggregates and faecal pellets were significantly reduced in the absence of *E. huxleyi* bloom formation (Fig. 3a), which can be attributed to lower $CaCO_3$ ballasting[23] (Fig. 3b–e). Reduced ballasting resulted in the lower rate of organic matter sedimentation in the high-CO_2 treatments (Fig. 4), which correlates with a lower vertical flux of $CaCO_3$ (Supplementary Fig. 4). The correlation of sinking velocity versus *E. huxleyi* abundance can serve to estimate
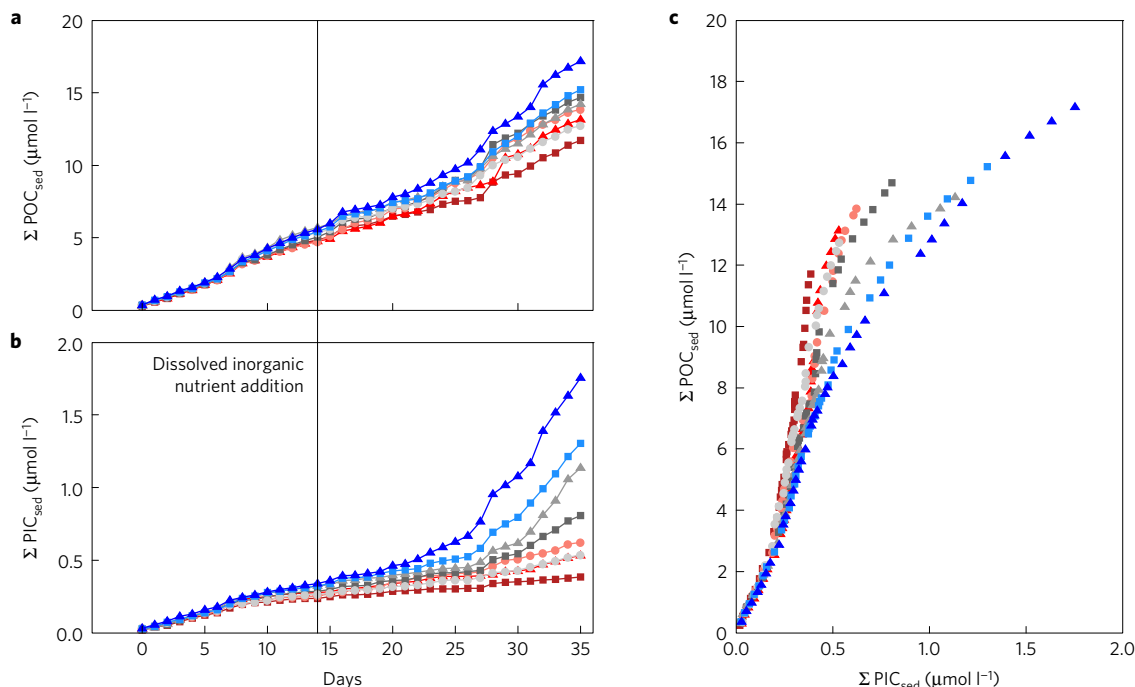
Figure 4 | Implications for vertical fluxes. a,b, Cumulative particulate organic carbon ($\sum POC_{sed}$) (**a**) and cumulative particulate inorganic carbon ($\sum PIC_{sed}$) (**b**) collected in the mesocosm sediment traps during the experiment. **c**, $\sum POC_{sed}$ versus $\sum PIC_{sed}$ over time. Colour code as in Fig. 1.

the potential for a change in organic matter transfer efficiency. The latter is defined as the ratio of sequestration flux (the amount of sinking matter reaching the bottom of the mesopelagic zone, that is, 1,000 m) to export flux (the amount passing through the bottom of the euphotic zone, that is, 100 m). Using a one-dimensional carbon flux model, a lowering of the transfer efficiency from 24% at coccolithophore abundances of 1,500 cells ml^{-1}, as observed in the control mesocosm, to 14% in the absence of coccolith ballasting, representative for the high CO_2 treatments, was calculated[23]. Although too limited in scope to be extrapolated to the global ocean, these results indicate the potential of reduced coccolithophore abundances in shoaling the remineralization depth, weakening the biological carbon pump and reducing oceanic carbon sequestration[24,25].

The CO_2-induced failure of *E. huxleyi* bloom formation also affected the production of dimethylsulfoniopropionate (DMSP) and its breakdown product dimethylsulfide (DMS) for which *E. huxleyi* is known to be one of the predominant producers in the ocean[26]. DMS concentrations were comparatively low during the first phase of the experiment (days 0–14), when *E. huxleyi* abundances were still low. As observed in previous CO_2 perturbation studies[27,28], DMS and dissolved and particulate DMSP displayed a slight negative correlation with p_{CO_2}. This negative correlation became much more pronounced during the second phase of the experiment, when DMSP and DMS were reduced in high- compared with low-CO_2 treatments by 30% and 60%, respectively[29]. This large difference closely correlates to the difference in *E. huxleyi* biomass between p_{CO_2} treatments[29]. When emitted from the ocean, DMS is considered to act as a cooling agent in the atmosphere[30]. Diminished DMS production due to a decline in *E. huxleyi* abundance under high p_{CO_2} may therefore exert a positive feedback to the climate system, potentially amplifying global warming[31].

The effects of ocean acidification on the physiology of *E. huxleyi* have been studied extensively in well-controlled laboratory experiments[12,32,33]. Yet, the information gained from these studies would not have led us to forecast the observed effects of CO_2-induced acidification on *E. huxleyi* in its natural environment. This highlights the need for more realistic community

and ecosystem-level experimentation to better understand the role of competitive and trophic interactions in climate-driven biological changes[34]. To what extent evolutionary adaptation is capable of alleviating these adverse effects of ocean acidification is currently uncertain. While *E. huxleyi* was able to partially restore its growth rate when adapted to high CO_2 for a few hundred generations[35], adaptation did not lead to full recovery of growth rates even after 1,500 generations[36].

A bottleneck for the future success of *E. huxleyi* may lie in maintaining seed population densities large enough to induce bloom formation. A small CO_2/pH-induced decline in growth rate can deteriorate *E. huxleyi*'s ability to maintain positive net growth during non-bloom seasons, which comprise most of the annual cycle. With most non-calcareous phytoplankton being either unaffected or stimulated by rising p_{CO_2}/declining pH[32], *E. huxleyi* may thereby lose its competitive fitness in an acidifying ocean. This would compromise its ability in the future ocean to maintain its cosmopolitan distribution and form the spectacular blooms occurring annually in large parts of the temperate and sub-polar oceans[14], covering sea surface areas of up to 250,000 km^2. A switch from coccolithophores to non-calcareous phytoplankton in these areas can initiate regime shifts, as previously seen in the Bering Sea[14], with potentially far-reaching ecological and biogeochemical consequences.

Methods

Methods, including statements of data availability and any associated accession codes and references, are available in the online version of this paper.

References

1. Brown, C. W. & Yoder, J. A. Coccolithophorid blooms in the global ocean. *J. Geophys. Res.* **99,** 7467–7482 (1994).
2. Young, J. R. in *Coccolithophores* (eds Winter, A. & Siesser, W. G.) 63–82 (Cambridge Univ. Press, 1994).

3. Raven, J. A. & Crawfurd, K. Environmental controls on coccolithophore calcification. *Mar. Ecol. Prog. Ser.* **470,** 137–166 (2012).
4. Broecker, W. & Clark, E. Ratio of coccolith $CaCO_3$ to foraminifera $CaCO_3$ in late Holocene deep sea sediments. *Paleoceanography* **24,** PA3205 (2009).
5. Tyrrell, T., Holligan, P. M. & Mobley, C. D. Optical impacts of oceanic coccolithophore blooms. *J. Geophys. Res.* **104,** 3223–3241 (1999).
6. Frankignoulle, M., Canon, C. & Gattuso, J.-P. Marine calcification as a source of carbon dioxide: positive feedback of increasing atmospheric CO_2. *Limnol. Oceanogr.* **39,** 458–462 (1994).
7. Armstrong, R. A., Lee, C., Hedges, J. I., Honjo, S. & Wakeham, S. G. A new, mechanistic model for organic carbon fluxes in the ocean based on the quantitative association of POC with ballast minerals. *Deep-Sea Res. II* **49,** 219–236 (2002).
8. Klaas, C. & Archer, D. A. Association of sinking organic matter with various types of mineral ballast in the deep sea: implications for the rain ratio. *Glob. Biogeochem. Cycles* **16,** 1116 (2002).
9. Bach, L. T., Riebesell, U., Gutowska, M. A., Federwisch, L. & Schulz, K. G. A unifying concept of coccolithophore sensitivity to changing carbonate chemistry embedded in an ecological framework. *Prog. Oceanogr.* **135,** 125–138 (2015).
10. Langer, G. *et al.* Species-specific responses of calcifying algae to changing seawater carbonate chemistry. *Geochem. Geophys. Geosyst.* **7,** Q09006 (2006).
11. Langer, G., Nehrke, G., Probert, I., Ly, J. & Ziveri, P. Strain specific responses of *Emiliania huxleyi* to changing seawater carbonate chemistry. *Biogeosciences* **6,** 2637–2646 (2009).
12. Meyer, J. & Riebesell, U. Responses of coccolithophores to ocean acidification: a meta-analysis. *Biogeosciences* **12,** 1671–1682 (2015).
13. IPCC *Climate Change 2014: Synthesis Report* (eds Pachauri, R. K. & Meyer, L. A.) (2014).
14. Tyrrell, T. & Merico, A. in *Coccolithophores: From Molecular Processes to Global Impact* (eds Thierstein, H. R. & Young, J. R.) 75–97 (Springer, 2004).
15. Delille, B. *et al.* Response of primary production and calcification to changes of p_{CO_2} during experimental blooms of the coccolithophorid *Emiliania huxleyi*. *Glob. Biogeochem. Cycles* **19,** GB2023 (2005).
16. Engel, A. *et al.* Testing the direct effect of CO_2 concentration on a bloom of the coccolithophorid *Emiliania huxleyi* in mesocosm experiments. *Limnol. Oceanogr.* **50,** 493–504 (2005).
17. Paulino, A. I., Egge, J. K. & Larsen, A. Effects of increased atmospheric CO_2 on small and intermediate sized osmotrophs during a nutrient induced phytoplankton bloom. *Biogeosciences* **5,** 739–748 (2008).
18. Schulz, K. G. *et al.* Build-up and decline of organic matter during PeECE III. *Biogeosciences* **5,** 707–718 (2008).
19. Hopkins, F. E. *et al.* Ocean acidification and marine trace gas emissions. *Proc. Natl Acad. Sci. USA* **107,** 760–765 (2010).
20. Feng, Y. *et al.* Interactive effects of increased p_{CO_2}, temperature and irradiance on the marine coccolithophore *Emiliania huxleyi* (Prymnesiophyceae). *Eur. J. Phycol.* **43,** 87–98 (2008).
21. Rokitta, S. D. & Rost, B. Effects of CO_2 and their modulation by light in the lifecycle stages of the coccolithophore *Emiliania huxleyi*. *Limnol. Oceanogr.* **57,** 607–618 (2012).
22. Zhang, Y., Bach, L. T., Schulz, K. G. & Riebesell, U. The modulating effect of light intensity on the response of the coccolithophore *Gephyrocapsa oceanica* to ocean acidification. *Limnol. Oceanogr.* **60,** 2145–2157 (2015).
23. Bach, L. T. *et al.* Influence of plankton community structure on the sinking velocity of marine aggregates. *Glob. Biogeochem. Cycles* **30,** 1145–1165 (2016).
24. Kwon, E. Y., Primeau, F. & Sarmiento, J. L. The impact of remineralisation depth on the air–sea carbon balance. *Nat. Geosci.* **2,** 630–635 (2009).
25. Riebesell, U., Körtzinger, A. & Oschlies, A. Sensitivities of marine carbon fluxes to ocean change. *Proc. Natl Acad. Sci. USA* **106,** 20602–20609 (2009).
26. Keller, M. D., Bellows, W. K. & Guillard, R. R. L. in *Biogenic Sulfur in the Environment* (eds Saltzman, E. S. & Cooper, W. J.) 167–183 (American Chemical Society, 1989).
27. Avgoustidi, V. *et al.* Decreased marine dimethyl sulfide production under elevated CO_2 levels in mesocosm and *in vitro* studies. *Environ. Chem.* **9,** 399–404 (2012).
28. Archer, S. D. *et al.* Contrasting responses of DMS and DMSP to ocean acidification in Arctic waters. *Biogeosciences* **10,** 1893–1908 (2013).
29. Webb, A. L. *et al.* The effect of ocean acidification on DMS and DMSP production from *Emiliania huxleyi* in laboratory and mesocosm studies. *Environm. Chem.* **13,** 314–329 (2015).
30. Levasseur, M. If Gaia could talk. *Nat. Geosci.* **4,** 351–352 (2011).
31. Six, K. D. *et al.* Global warming amplified by reduced sulphur fluxes as a result of ocean acidification. *Nat. Clim. Change* **3,** 975–978 (2013).
32. Riebesell, U. & Tortell, P. D. in *Ocean Acidification* (eds Gattuso, J.-P. & Hansson, L.) 99–121 (Oxford Univ. Press, 2011).
33. Zondervan, I. The effect of light, macronutrients, trace metals and CO_2 on the production of calcium carbonate and organic carbon in coccolithophores—a review. *Deep-Sea Res. II* **41,** 521–537 (2007).
34. Stewart, R. I. A. *et al.* Mesocosm experiments as tool for ecological climate-change research. *Adv. Ecol. Res.* **48,** 71–181 (2013).
35. Lohbeck, K. T., Riebesell, U., Collins, S. & Reusch, T. B. H. Adaptive evolution of a key phytoplankton species to ocean acidification. *Nat. Geosci.* **5,** 346–352 (2012).
36. Lohbeck, K. T., Riebesell, U., Collins, S. & Reusch, T. B. H. Functional genetic divergence in high CO_2 adapted *Emiliania huxleyi* populations. *Evolution* **67,** 1892–1900 (2012).
37. Wessa, P. *Pearson Correlation in Free Statistics Software* (Office for Research Development and Education, 2015); http://www.wessa.net/rwasp_correlation.wasp

Author contributions

U.R. designed and coordinated the experiment and wrote the manuscript. U.R., L.T.B., J.R.B.M., T.B., J.C., A.Ludwig and K.G.S. carried out the mesocosm experiment. R.G.J.B. measured A_T and C_T. K.G.S. measured pH and calculated carbonate chemistry. A.Larsen measured *E. huxleyi* cell abundances. A.Ludwig measured chlorophyll *a* and inorganic nutrient concentrations. L.T.B. measured particle sinking rates and took scanning electron micrographs. J.R.B.M. determined phytoplankton composition and abundances. T.B. measured sedimentation rates. All authors contributed to the data analysis, discussed the results and commented on the manuscript.

Additional information

Supplementary information is available in the online version of the paper. Reprints and permissions information is available online at www.nature.com/reprints. Correspondence and requests for materials should be addressed to U.R.

Competing financial interests

The authors declare no competing financial interests.

Methods

Experimental setup. On 30 April 2011, nine 25-m-long, pelagic mesocosm units of the Kiel Off-Shore Mesocosms for Future Ocean Simulations (KOSMOS) were deployed in the Raunefjord, west coast of Norway at 60.265° N, 5.205° E at a water depth of 55 to 65 m. A detailed description of the experimental setup, its deployment, technical features and the sampling methods are described in refs 38,39. The flexible thermoplastic polyurethane bags, each enclosing about 75 m^3 of seawater, were filled on 1 May and closed off from exchange with the surrounding water three days later. After 4 days of measurements of some core parameters to check for identical starting conditions in all mesocosms, manipulation of the seawater carbonate chemistry began on 8 May (termed day 0). Seven mesocosms were adjusted over five days to target p_{CO_2} levels of ~400 (M6), ~600 (M8), ~900 (M1), ~1,200 (M3), ~1,300 (M5), ~2,000 (M7) and ~3,000 (M9) µatm by stepwise additions of CO_2-saturated seawater. Two mesocosms (M2, M4) were used as control treatments at *in situ* p_{CO_2} of approximately 300 µatm. CO_2 treatments were arranged in an assorted design of the mesocosms in relation to each other and the shore to avoid that external variation (for example, light or salinity gradients) could bias our treatment effects (Supplementary Fig. 1). The inside of the mesocosm walls was cleaned regularly with a ring-shaped, double-bladed wiper to prevent biofilm growth[38]. After termination of the experiment, one small hole was detected in the bag of M2, which had led to non-quantifiable water exchange. This mesocosm was therefore excluded from further analyses.

Sampling of the mesocosms and the surrounding fjord with a depth-integrating water sampler (0–23 m depth, Hydrobios Kiel) started on 7 May and was carried out daily for 35 days until 12 June. On day 14, 5 µmol l^{-1} nitrate and 0.16 µmol l^{-1} phosphate were added to the mesocosms. The average pH_T before nutrient addition ranged between pH_T 8.13 ± 0.01 in the control mesocosms and pH_T 7.31 ± 0.12 in the highest p_{CO_2} mesocosm. After nutrient addition, pH_T ranged between pH_T 8.14 ± 0.01 in the control mesocosms and pH_T 7.49 ± 0.05 in the highest p_{CO_2} mesocosm. Temperature varied between 6.8 °C at the beginning and 10.0 °C at the end of the experiment.

Measurements of dissolved inorganic carbon, pH and total alkalinity. Total pH(pH_T) was measured spectrophotometrically with a VARIAN Cary 100 in a 10 cm cuvette at 25 °C as described in ref. 40 and then recalculated to *in situ* temperature. The precision was typically better than 0.001 at high and 0.002 at low pH_T. Total alkalinity (A_T) was measured using Gran potentiometric titration on a VINDTA system[41] with a precision of 2 µmol kg^{-1}. Dissolved inorganic carbon (C_T) was determined using coulometric titration[42] with a precision of ≤2 µmol kg^{-1}. Measurements for both C_T and A_T were calibrated against certified reference material[43]. p_{CO_2} was calculated for *in situ* temperatures and salinities from measured dissolved inorganic carbon and pH_T (at 25 °C) using the stoichiometric equilibrium constants for carbonic acid of ref. 44 as refitted by ref. 45.

Chlorophyll *a* analysis. For chlorophyll *a* analysis, 250–500 ml samples were filtered onto Whatman GF/F filters. Filters were stored at −80 °C for at least 24 h and then homogenized with 90% acetone and glass beads (2 and 4 mm) in a cell mill. After centrifugation, chlorophyll *a* concentrations were measured on a WATERS high-performance liquid chromatograph (HPLC) equipped with a Varian Microsorb-MV 100-3 C8 column according to ref. 46.

Flow cytometry. Phytoplankton less than approximately 15–20 µm were enumerated using a FacsCalibur flow cytometer (Becton Dickinson) equipped with an air-cooled laser providing 15 mW at 488 nm with standard filter setup. The phytoplankton counts were obtained from fresh samples with the trigger set on red fluorescence[47]. Discrimination of the various phytoplankton groups was based on dot plots of side-scatter signal versus pigment autofluorescence (chlorophyll and phycoerythrin).

Sedimentation. The quantitatively collecting sediment traps, built as an elongation of the cylindrical mesocosm bags[38], were emptied on a daily basis from 8 May until the last day of experiment, 12 June. Small subsamples of the particle suspensions were provided for the measurement of aggregate sinking velocities. Residual material was concentrated, lyophilized and ground to a homogeneous fine powder[48]. Carbon content of the material was analysed from subsamples of 2 mg

with an elemental analyser (Euro EA–CN, HEKAtech GmbH), whereas inorganic carbon was removed by direct addition of 50 µl 1 M HCl to measure the organic carbon fraction. Inorganic carbon was than calculated from total and organic carbon content.

Sinking rate. Aggregate sinking velocities of sediment trap material were determined on a daily basis until day 29 with an automated video camera setup (FlowCAM, Fluid imaging) as described in detail in ref. 49. Measurements were conducted on particles in the size range of 150–400 µm equivalent spherical diameter collected from sediment traps during the bloom period (days 25–29) and on faecal pellets obtained from triplicate bottle incubations of nutrient-enriched mesocosm water taken from mesocosms M4 (control), M1 (initial p_{CO_2} ~ 900 µatm) and M7 (initial p_{CO_2} ~ 2,000 µatm). After four days of incubation, copepods were added and allowed to graze for 24 h on the phytoplankton community, before faecal pellets were collected and their sinking velocities measured.

Statistical analyses. Relationships of p_{CO_2} with *E. huxleyi* net growth rate and cell abundance (Fig. 2) were tested by means of Pearson correlation (ref. 37). Relationships of *E. huxleyi* abundance with particle sinking velocity (Fig. 3) as well as of p_{CO_2} with cumulative sedimented POC and PIC (Supplementary Fig. 3) were tested with linear regression analysis using R (R Project for Statistical Computation). Regressions of p_{CO_2} with chlorophyll *a* during certain phases of the experiment were analysed with *F*-tests using phase averages.

Data availability. The authors declare that the data supporting the findings of this study are available within the article and its Supplementary Information files. The data from this mesocosm study are available via the following link: https://doi.pangaea.de/10.1594/PANGAEA.868772.

References

38. Riebesell, U. *et al*. Technical Note: A mobile sea-going mesocosm system—new opportunities for ocean change research. *Biogeosciences* **10,** 1835–1847 (2013).
39. Schulz, K. G. *et al*. Temporal biomass dynamics of an Arctic plankton bloom in response to increasing levels of atmospheric carbon dioxide. *Biogeosciences* **10,** 161–180 (2013).
40. Dickson, A. G. in *Guide to Best Practise in Ocean Acidification Research and Data Reporting* (eds Riebesell, U., Fabry, V. J., Hansson, L. & Gattuso, J.-P.) 17–40 (Luxembourg, 2010).
41. Mintrop, L., Fernández-Pérez, F., González Dávila, M., Körtzinger, A. & Santana Casiano, J. M. Alkalinity determination by potentiometry—intercalibration using three different methods. *Cienc. Mar.* **26,** 23–37 (2000).
42. Johnson, K. M., Sieburth, J. M., Williams, P. J. & Brandström, L. Coulometric total carbon analysis for marine studies: automation and calibration. *Mar. Chem.* **21,** 117–133 (1987).
43. Dickson, A. G. Standards for ocean measurements. *Oceanography* **23,** 34–47 (2010).
44. Mehrbach, C., Culberson, C. H., Hawley, J. E. & Pytkowicz, R. M. Measurements of the apparent dissociation constants of carbonic acid in seawater at atmospheric pressure. *Limnol. Oceanogr.* **18,** 897–907 (1973).
45. Lueker, T. J., Dickson, A. G. & Keeling, C. D. Ocean p_{CO_2} calculated from dissolved inorganic carbon, alkalinity, and equations for K_1 and K_2: validation based on laboratory measurements of CO_2 in gas and seawater at equilibrium. *Mar. Chem.* **70,** 105–119 (2000).
46. Barlow, R. G., Cummings, D. G. & Gibb, S. W. Improved resolution of mono- and divinyl chlorophylls *a* and *b* and zeaxanthin and lutein in phytoplankton extracts using reverse phase C-8 HPLC. *Mar. Ecol. Prog. Ser.* **161,** 303–307 (1997).
47. Larsen, A. *et al*. Population dynamics and diversity of phytoplankton, bacteria and viruses in a seawater enclosure. *Mar. Ecol. Prog. Ser.* **221,** 47–57 (2001).
48. Boxhammer, T., Bach, L. T., Czerny, J. & Riebesell, U. Technical Note: Sampling and processing of mesocosm sediment trap material for quantitative biogeochemical analysis. *Biogeosciences* **13,** 2849–2858 (2016).
49. Bach, L. T. *et al*. An approach for particle sinking velocity measurements in the 3–400 µm size range and considerations on the effect of temperature on sinking rates. *Mar. Biol.* **159,** 1853–1864 (2012).